

Single-Crystal-to-Single-Crystal Transformation in Unusual Three-Dimensional Manganese(II) Frameworks Exhibiting Unprecedented Topology and Homospin Ferrimagnet

Jiong-Peng Zhao, Bo-Wen Hu, Qian Yang, Tong-Liang Hu, and Xian-He Bu*

Department of Chemistry, Nankai University, Tianjin 300071, People's Republic of China

Received January 22, 2009

A new three-dimensional Mn^{II} complex, [Mn₃(HCO₂)₂(L)₂(OCH₃)₂], **1** (L = nicotinate *N*-oxide), was synthesized by solvothermal reaction and magnetically characterized. Complex **1** exhibits an unprecedented 3,6-connected 5-nodal net topology with Schläfli notation {4²;6}4{4³}₂{4⁶;6⁶;8³;10}₂{4⁸;6⁶;8} and was assigned as a homospin ferrimagnet. Interestingly, when **1** was placed in air for ca. one month, the methoxy anions in **1** were gradually exchanged by hydroxyl anions and **1** underwent a single-crystal-to-single-crystal structural transition to a new but similar complex, [Mn₃(HCO₂)₂(L)₂(OH)₂]·4H₂O, **2**. The anion exchange and water molecules filling the channels of **2** affect the magnetic behavior at low temperature compared to that of **1**.

Introduction

In recent years, considerable attention has been focused on the design and synthesis of molecular magnetic materials, for understanding fundamental magnetic interactions and magnetostructural correlations as well as the development of new molecule-based materials.¹ In particular, molecular magnetic materials with big and permanent spontaneous magnetization are continuously pursued for their potential application as molecular magnets.² However, it is still a big challenge to design and prepare such ferromagnets due to the weakness of the ferromagnetic interaction compared to the antiferromagnetic interaction.³ The “ferrimagnetic” strategy has been drawing more attention to realize the permanent magnetization due to the noncancellation of the antiferromagnetic coupled spins.⁴ The homospin ferrimagnetic systems containing only one type of spin carrier are more uncommon because

they need the particular spatial arrangement of the spins.⁵ It should also be pointed out that among the reported homospin ferrimagnetic systems, complexes with open framework structure are still rare.⁶ The construction of such magnetic materials has drawn much attention since the magnetism may be accommodated by altering the guest molecules, ligands, or metal ions in the open frameworks.⁷ Several single-crystal-to-single-crystal (SCSC) transformations were found in the ferrimagnetic systems.^{6,8} However, the most SCSC transformations were realized by dehydration/hydration. The SCSC transformations accompanied with anion exchange were scarce, especially in the 3D ferrimagnetic systems.

Carboxylate, as a bridging ligand, displaying multiple bridging modes, and being able to mediate magnetic coupling

*To whom correspondence should be addressed. E-mail: buxh@nankai.edu.cn. Fax: +86-22-23502458. Tel: +86-22-23502809.

(1) For examples: (a) Turnbull, M. M.; Sugimoto, T.; Thompson, L. K. *Molecule-Based Magnetic Materials*; American Chemical Society: Washington, DC, 1996. (b) Sakamoto, M.; Manseki, K.; Okawa, H. *Coord. Chem. Rev.* **2001**, *219–221*, 379. (c) Miller, J. S.; Drillon, M. *Magnetism: Molecules to Materials*; Wiley-VCH: Weinheim, 2001–2005. (d) Du, M.; Bu, X.-H.; Guo, Y.-M.; Ribas, J. *Chem.—Eur. J.* **2004**, *10*, 1345. (e) Zeng, Y.-F.; Hu, X.; Liu, F.-C.; Bu, X.-H. *Chem. Soc. Rev.* **2009**, *38*, 469.

(2) For examples: (a) Castillo, O.; Luque, A.; Román, P.; Lloret, F.; Julve, M. *Inorg. Chem.* **2001**, *40*, 5526. (b) Lu, Y.-B.; Wang, M.-S.; Zhou, W.-W.; Xu, G.; Guo, G.-C.; Huang, J.-S. *Inorg. Chem.* **2008**, *47*, 8935. (c) Wang, X.-Y.; Wang, Z.-M.; Gao, S. *Chem. Commun.* **2008**, 281.

(3) Wang, X.-Y.; Wang, Z.-M.; Gao, S. *Inorg. Chem.* **2008**, *47*, 5720.

(4) For examples: (a) Kahn, O.; Pei, Y.; Verdaguer, M.; Renard, J. P.; Sletten, J. *J. Am. Chem. Soc.* **1988**, *110*, 782. (b) Holmes, M. S.; Girolami, G. S. *J. Am. Chem. Soc.* **1999**, *121*, 5593. (c) Manriquez, J. M.; Yee, G. T.; Mclean, R. S.; Epstein, A. J.; Miller, J. S. *Science* **1991**, *252*, 1415. (d) Ferlay, S.; Mallah, T.; Quahes, R.; Veillet, P.; Verdaguer, M. *Nature* **1995**, *378*, 701.

(5) For examples: (a) Escuer, A.; Vicente, R.; Fallah, M. S. E.; Goher, M. A. S.; Mautner, F. A. *Inorg. Chem.* **1998**, *37*, 4466. (b) Abu-Youssef, M. A. M.; Drillon, M.; Escuer, A.; Goher, M. A. S.; Mautner, F. A.; Vicente, R. *Inorg. Chem.* **2000**, *39*, 5022. (c) Abu-Youssef, M. A. M.; Escuer, A.; Goher, M. A. S.; Mautner, F. A.; Reib, G. J.; Vicente, R. *Angew. Chem., Int. Ed.* **2000**, *39*, 1624. (d) Gao, E.-Q.; Yue, Y.-F.; Bai, S.-Q.; He, Z.; Yan, C.-H. *J. Am. Chem. Soc.* **2004**, *126*, 1419.

(6) (a) Wang, Z.-M.; Zhang, B.; Fujiwara, H.; Kobayashi, H.; Kurmoo, M. *Chem. Commun.* **2004**, 416. (b) Wang, X.-Y.; Scancella, M.; Sevov, S. C. *Chem. Mater.* **2007**, *19*, 4506.

(7) For examples: (a) Milon, J.; Daniel, M.-C.; Kaiba, A.; Guionneau, P.; Brandès, S.; Sutter, J.-P. *J. Am. Chem. Soc.* **2007**, *129*, 13872. (b) Wang, Z.-M.; Zhang, B.; Kurmoo, M.; Green, M. A.; Fujiwara, H.; Otsuka, T.; Kobayashi, H. *Inorg. Chem.* **2005**, *44*, 1230. (c) Ouellette, W.; Prosvirin, A. V.; Whitenack, K.; Dunbar, K. R. *Angew. Chem., Int. Ed.* **2009**, *48*, 1. (d) Maspoch, D.; Ruiz-Molina, D.; Wurst, K.; Domingo, N.; Cavallini, M.; Biscarini, F.; Tejada, J.; Rovira, C.; Veciana, J. *Nat. Mater.* **2003**, *2*, 190. (e) Maspoch, D.; Ruiz-Molina, D.; Veciana, J. *Chem. Soc. Rev.* **2007**, *36*, 770.

(8) (a) Kaneko, M.; Ohba, M.; Kitagawa, S. *J. Am. Chem. Soc.* **2007**, *129*, 13706. (b) Nowicka, B.; Rams, M.; Stadnicka, K.; Sieklucka, B. *Inorg. Chem.* **2007**, *46*, 8123. (c) Yoshida, Y.; Inoue, K.; Kurmoo, M. *Inorg. Chem.* **2009**, *48*, 267.

effectively between metal ions, has been well used in preparing molecular magnetic materials.⁹ Numerous magnetic materials exhibiting diverse bulk magnetic behaviors such as antiferromagnetism, ferromagnetism, spin crossover, spin canting, and ferrimagnetism¹⁰ were constructed based on different carboxylates including formate.^{6a,7b,11} With respect to complexes containing carboxylate ligands with auxiliary ligands, quite a few magnetic systems including two types of carboxylates, especially the smallest carboxylate, the formate anion, have been characterized.¹² New complexes with diverse structures and particular properties may be obtained by using another carboxylate to partially substitute the formate anions in the metal formates. However, arbitrarily replacing the formate anions by other carboxylates in the metal formates is still a challenge. The powerful solvothermal technique in growing new crystals may be effective in this system.

Herein, we report a formate-bridged complex, $[\text{Mn}_3(\text{HCO}_2)_2(\text{L})_2(\text{OCH}_3)_2]$ (**1**), with the auxiliary ligand **L** (**L** = nicotinate *N*-oxide) and another short bridging methoxy ligand. The 3D structure of **1** is formed by formate/carboxylate/methoxy mixed-bridged Mn^{II} chains linked by the **L** ligands. Long-range ordering was found to be present in **1**, which was assigned as a homospin ferrimagnet. Interestingly, by placing **1** in air for ca. one month, a single-crystal-to-single-crystal structural transition from **1** to a new but similar complex, $[\text{Mn}_3(\text{HCO}_2)_2(\text{L})_2(\text{OH})_2] \cdot 4\text{H}_2\text{O}$ (**2**), was observed. A magnetic study indicated that the anion exchange and water molecules filling the channels of **2** increased the phase transition temperature of the magnetic order compared to that of **1**.

Experimental Section

Materials and Physical Measurements. All the chemicals used for synthesis are of analytical grade and commercially available. Nicotinate *N*-oxide acid, formate acid, manganese carbonate, and methanol were purchased from commercial sources and used as received. $\text{Mn}(\text{HCO}_2)_2 \cdot 4\text{H}_2\text{O}$ was synthesized by dissolving manganese carbonate in formic acid and concentrating. The solid product was separated by filtration.

Elemental analyses (C, H, N) were performed on a Perkin-Elmer 240C elemental analyzer. IR spectra were measured on a Tensor 27 OPUS (Bruker) FT-IR spectrometer with KBr pellets. The X-ray powder diffraction (XRPD) was recorded on a Rigaku D/Max-2500 diffractometer at 50 kV, 40 mA for a Cu-

target tube, and a graphite monochromator. Simulation of the XRPD spectra was carried out by the single-crystal data and diffraction-crystal module of the Mercury (Hg) program available free of charge via the Internet at <http://www.iucr.org>.

Magnetic data were collected using crushed crystals of the sample on a Quantum Design MPMS-XL SQUID magnetometer equipped with a 5 T magnet. The data were corrected using Pascal's constants to calculate the diamagnetic susceptibility, and an experimental correction for the sample holder was applied.

Synthesis. A mixture of $\text{Mn}(\text{HCO}_2)_2 \cdot 4\text{H}_2\text{O}$ and **L** (**L** = nicotinate *N*-oxide) at a ratio of 1:0.75 in 15 mL of methanol was sealed in a Teflon-lined stainless steel vessel, heated at 140 °C for 2 days under autogenous pressure, and then cooled to room temperature. Yellow crystals of **1** were harvested in ca. 20% yield based on $\text{Mn}(\text{HCO}_2)_2 \cdot 4\text{H}_2\text{O}$. For the IR spectra of **1**, see Figure S1. Anal. Calcd for $\text{C}_{16}\text{H}_{16}\text{Mn}_3\text{N}_2\text{O}_{12}$: C, 32.40; H, 2.72; N, 4.72. Found: C, 31.97; H, 3.10; N, 4.30. By placing **1** in air with suitable humidity for ca. one month a single-crystal-to-single-crystal structural transition from **1** to **2** occurred. The water molecules in the air may diffuse into the channels gradually and replace the coordinating methoxy anions in **1** to form coordinating hydroxyl anions and methanols that diffused into the air. Finally, all the methoxy anions in **1** were replaced by hydroxyl anions, and the channels were filled with water molecules completely, forming a similar but new complex, **2**, which was confirmed by X-ray structure analysis. For the IR spectra of **2**, see Figure S1. Anal. Calcd for $\text{C}_{14}\text{H}_{20}\text{Mn}_3\text{N}_2\text{O}_{16}$: C, 26.39; H, 3.16; N, 4.40. Found: C, 26.74; H, 2.80; N, 4.75.

Complex **1** could remain considerably stable in a dry environment (the complex remained unchanged over one month when placed in a desiccator with a dryer, which was confirmed by X-ray structural analysis), and the transformation from **1** to **2** took place only when **1** was left in air with suitable humidity. The transformation process took about one month in air with ca. 50% relative humidity. However, complex **1** decomposed when it was placed in saturated steam in about two days. Our attempts to synthesize complex **2** by a hydrothermal method directly were not successful.

X-ray Data Collection and Structure Determinations. X-ray single-crystal diffraction data for complexes **1** and **2** were collected on a Rigaku SCX-mini diffractometer at 293(2) K with Mo $K\alpha$ radiation ($\lambda = 0.71073 \text{ \AA}$) by ω scan mode. The program SAINT¹³ was used for integration of the diffraction profiles. All the structures were solved by direct methods using the SHELXS program of the SHELXTL package and refined by full-matrix least-squares methods with SHELXL (semiempirical absorption corrections were applied using the SADABS program).¹⁴ Metal atoms in each complex were located from the *E*-maps, and other non-hydrogen atoms were located in successive difference Fourier syntheses and refined with anisotropic thermal parameters on F^2 . The hydrogen atoms of the ligands were generated theoretically onto the specific atoms and refined isotropically with fixed thermal factors. Detailed crystallographic data are summarized in Table 1.

Results and Discussion

Description of Crystal Structure. Single-crystal X-ray diffraction analysis of the light yellow crystals of **1** reveals a 3D coordination network crystallizing in the space group *C2/c*. The asymmetric unit contains one and a half Mn^{II} ions, one formate anion, one **L** ligand, and one deprotonated methanol. Mn1 is coordinated by six oxygen atoms from two methoxy anions, two formate anions,

(9) For examples: (a) Mukherjee, P. S.; Dalai, S.; Mostafa, G.; Zangrando, E.; Lu, T.-H.; Rogez, G.; Mallah, T.; Ray Chaudhuri, N. *Chem. Commun.* **2001**, 1346. (b) Eddaoudi, M.; Moler, D. B.; Li, H.; Chen, B.; Reineke, T. M.; O'Keeffe, M.; Yaghi, O. M. *Acc. Chem. Res.* **2001**, *34*, 319. (c) Du, M.; Bu, X.-H.; Guo, Y.-M.; Zhang, L.; Liao, D.-Z.; Ribas, J. *Chem. Commun.* **2002**, 1478. (d) Chui, S. S.-Y.; Lo, S. M.-F.; Charmant, J. P. H.; Orpen, A. G.; Williams, I. D. *Science* **1999**, *238*, 1148. (e) Deacon, G. B.; Phillips, R. J. *Coord. Chem. Rev.* **1980**, *33*, 227.

(10) For examples: (a) Konar, S.; Mukherjee, P. S.; Drew, M. G. B.; Ribas, J.; Chaudhuri, N. R. *Inorg. Chem.* **2003**, *42*, 2545. (b) Ruiz-Pérez, C.; Sanchiz, J.; Molina, M. H.; Lloret, F.; Julve, M. *Inorg. Chem.* **2000**, *39*, 1363. (c) Armentano, D.; Munno, G. D.; Mastropietro, T. F.; Proserpio, D. M.; Julve, M.; Lloret, F. *Inorg. Chem.* **2004**, *43*, 5177. (d) Kumagai, H.; Kepert, C. J.; Kurmoo, M. *Inorg. Chem.* **2002**, *41*, 3410. (e) Zeng, M.-H.; Zhang, W.-X.; Sun, X.-Z.; Chen, X.-M. *Angew. Chem., Int. Ed.* **2005**, *44*, 2.

(11) For examples: (a) Wang, X.-Y.; Wang, Z.-M.; Gao, S. *Chem. Commun.* **2007**, 1127. (b) Viertelhaus, M.; Henke, H.; Anson, C. E.; Powell, A. K. *Eur. J. Inorg. Chem.* **2003**, 2283. (c) Viertelhaus, M.; Adler, P.; Clérac, R.; Anson, C. E.; Powell, A. K. *Eur. J. Inorg. Chem.* **2005**, 692. (d) Wang, X.-Y.; Lin, C.; Zhang, S.-W.; Gao, S. *Inorg. Chem.* **2004**, *43*, 4615.

(12) Zhang, J.; Chen, S.; Valle, H.; Wong, A. M. C.; Cruz, M.; Bu, X.-H. *J. Am. Chem. Soc.* **2007**, *129*, 14168.

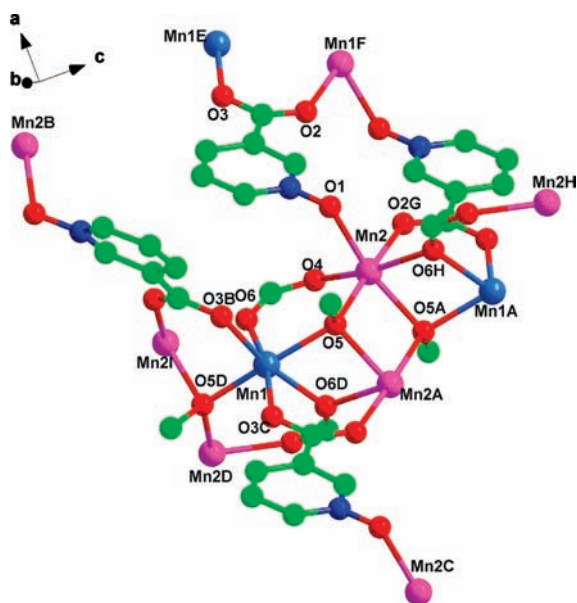
(13) Bruker A. X. S. *SAINT Software Reference Manual*; Madison, WI, 1998.

(14) Sheldrick, G. M. *SHELXTL NT Version 5.1, Program for Solution and Refinement of Crystal Structures*; University of Göttingen: Germany, 1997.

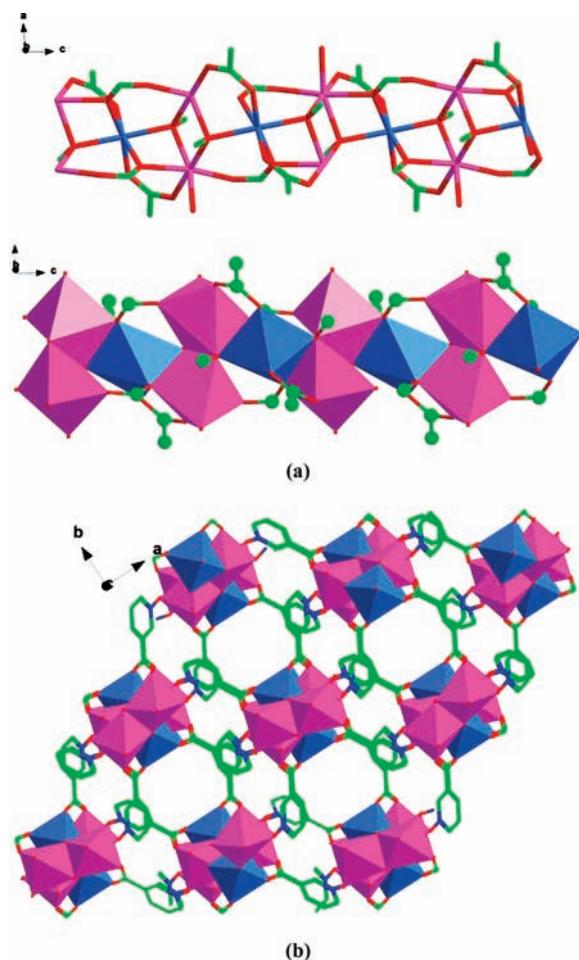
Table 1. Crystal Data and Structure Refinement Parameters for Complexes **1** and **2**

	1	2
chemical formula	C ₁₆ H ₁₆ Mn ₃ N ₂ O ₁₂	C ₁₄ H ₂₀ Mn ₃ N ₂ O ₁₆
fw	593.13	637.14
space group	C2/c	C2/c
<i>a</i> /Å	17.993(4)	17.334(3)
<i>b</i> /Å	10.644(2)	11.183(2)
<i>c</i> /Å	11.531(2)	11.418(2)
β /deg	91.23(3)	95.96(3)
<i>V</i> /Å ³	2208.0(8)	2201.4(7)
<i>Z</i>	4	4
<i>D</i> /g cm ⁻³	1.722	1.922
μ /mm ⁻¹	1.816	1.779
<i>T</i> /K	293(2)	293(2)
<i>R</i> ^a / <i>wR</i> ^b	0.0273/0.0616	0.0360/0.0677

$$^a R = \sum ||F_o| - |F_c|| / \sum |F_o|. \quad ^b R_w = [\sum [w(F_o^2 - F_c^2)^2] / \sum w(F_o^2)]^{1/2}.$$

**Figure 1.** Coordination and linkage modes of the ligands and Mn^{II} ions in **1**.

and two carboxylates of **L** ligands (Figure 1). Mn2 is coordinated by two methoxy oxygen atoms, one carboxylate oxygen atom, two formate oxygen atoms, and one oxygen atom from the *N*-oxide group of **L** ligand. The methoxy ligand takes a μ_3 coordination mode bridging three Mn^{II} ions with the bond angles Mn1–O5–Mn2A = 98.93°, Mn1–O5–Mn2 = 118.32°, and Mn2–O5–Mn2A = 95.89°. The distances of the Mn^{II} ions bridged by the methoxy are Mn1...Mn2 = 3.785 Å, Mn1...Mn2A = 3.342 Å, and Mn2...Mn2 = 3.242 Å. The **L** ligand bridges three Mn^{II} ions using the oxygen atoms of *N*-oxide and the *syn,syn* carboxylate group. The formate taking the frequent *syn,syn,anti* mode links three Mn^{II} ions with a Mn1–O6–Mn2I bond angle of 96.9°. Thus a formate/carboxylate/methoxy mixed-bridged Mn^{II} chain is formed (Figure 2a). The structural and magnetic topology of the chain is very similar to that reported by Dietzel.¹⁵ The 3D structure of **1** can be described as formate/carboxylate/methoxy mixed-bridged Mn^{II} chains linked by **L** ligands (Figure 2b). It is interesting

**Figure 2.** (a) Formate/carboxylate/methoxy mixed bridged Mn^{II} 1D chain in **1**. (b) Polyhedron view of the 3D structure of **1**.

that a 1D channel is formed along the *c* direction (Figure S2) in **1**. In the structure of **1**, each anion linking three metal ions can be considered as 3-connecting nodes and the metal ions as 6-connected nodes. The 3D net can be viewed as a 3,6-connected 5-nodal net with Schläfli notation {4²;6}4{4³}2{4⁶;6⁶;8³;10}2{4⁸;6⁶;8} (Figure 3). To the best of our knowledge, such a net is unprecedented.¹⁶

The structures of **2** and **1** are nearly the same except for the hydroxyl anions replacing the methoxy anions and a small amount of waters filling the channels. The key bond lengths and angles of **2** have small differences from that of **1** (see Table 2). The two types of water molecules of the asymmetric unit in **2** are stabilized by the hydrogen bonds forming a (H₂O)₄ structure (Figure 4) in the 1D channels of **2**. On the basis of PLATON analysis,¹⁷ approximately 17.3% of the crystal volume (2201 Å³) is occupied by lattice water molecules with a volume of 380 Å³ in each unit cell of **2**. That is larger than the guest free channel in **1**, with a volume of 149 Å³, because the hydroxyl anions are much smaller than the methoxy group (Figure S2).

(16) (a) Reticular Chemistry Structure Resource (RCSR), <http://rcsr.anu.edu.au/>. (b) Euclidean Patterns in Non-Euclidean Tilings (EPINET), <http://epinet.anu.edu.au/>. (c) Blatov, V. A.; Shevchenko, A. P. *TOPOS 4.0*; Samara State University: Russia.

(17) Spek, A. L. *PLATON, A Multipurpose Crystallographic Tool*; Utrecht University: Utrecht, The Netherlands, 1999.

(15) Dietzel, P. D. C.; Morita, Y.; Blom, R.; Fjellvåg, H. *Angew. Chem., Int. Ed.* **2005**, *44*, 6354.

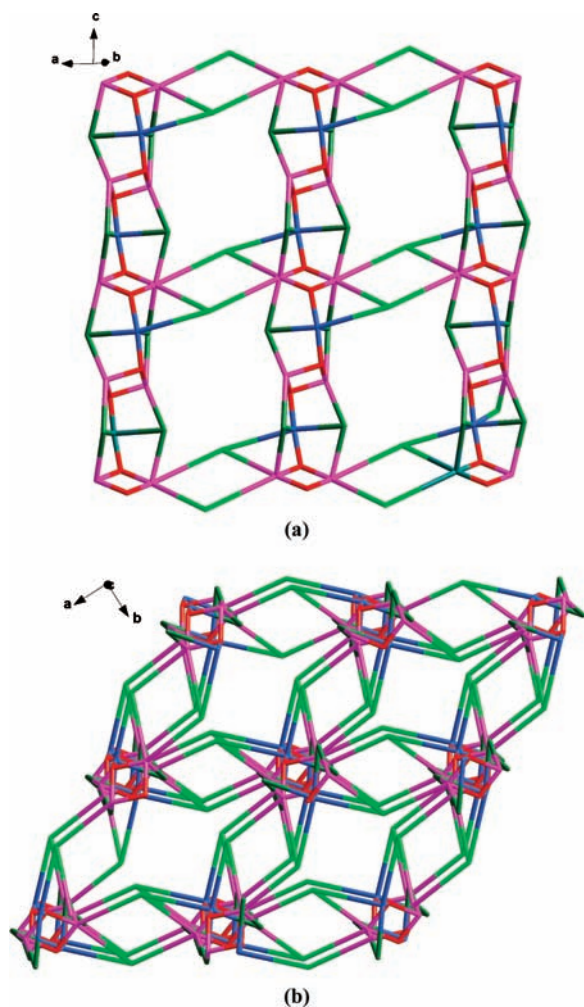


Figure 3. (a) Layer views of the network topology in **1**. (b) Views of the network topology of **1**.

Table 2. Selected Bond Lengths [Å] and Angles for Complexes **1** and **2** [deg]^a

1		2	
Mn(1)–O(3)#2	2.148(4)	Mn(1)–O(3)#2	2.191(2)
Mn(1)–O(3)#3	2.148(4)	Mn(1)–O(3)#3	2.191(2)
Mn(1)–O(5)#4	2.220(4)	Mn(1)–O(5)#4	2.180(2)
Mn(1)–O(6)#4	2.193(4)	Mn(1)–O(6)#4	2.246(2)
Mn(1)–O(6)	2.193(4)	Mn(1)–O(6)	2.246(2)
Mn(1)–O(5)	2.220(4)	Mn(1)–O(5)	2.180(2)
Mn(2)–O(6)#7	2.193(4)	Mn(2)–O(6)#7	2.248(2)
Mn(2)–O(5)#1	2.178(4)	Mn(2)–O(5)#1	2.187(2)
Mn(2)–O(4)	2.146(5)	Mn(2)–O(4)	2.190(2)
Mn(2)–O(1)	2.173(5)	Mn(2)–O(1)	2.168(2)
Mn(2)–O(2)#6	2.220(4)	Mn(2)–O(2)#6	2.185(2)
Mn(2)–O(5)	2.178(4)	Mn(2)–O(5)	2.172(2)
Mn(2)#1–O(5)–Mn(2)	95.89(17)	Mn(2)#1–O(5)–Mn(2)	96.17(9)
Mn(2)#1–O(5)–Mn(1)	98.93(17)	Mn(2)#1–O(5)–Mn(1)	100.46(10)
Mn(2)–O(5)–Mn(1)	118.32(19)	Mn(2)–O(5)–Mn(1)	122.06(11)
Mn(1)–O(6)–Mn(2)#8	98.46(18)	Mn(1)–O(6)–Mn(2)#8	96.67(8)

^a #1 $-x, -y+1, -z+2$; #2 $-x+1/2, y+1/2, -z+3/2$; #3 $x-1/2, y+1/2, z$; #4 $-x, y, -z+3/2$; #6 $-x+1/2, -y+1/2, -z+2$; #7 $x, -y+1, z+1/2$; #8 $x, -y+1, z-1/2$.

The structural consistency and phase purity of **1** and **2** were confirmed by comparing the measured patterns calculated from single-crystal data with the experimental X-ray powder diffraction (XRPD) analysis at room temperature (Figure 5). That also indicated the transformation from **1** to **2** is completed.

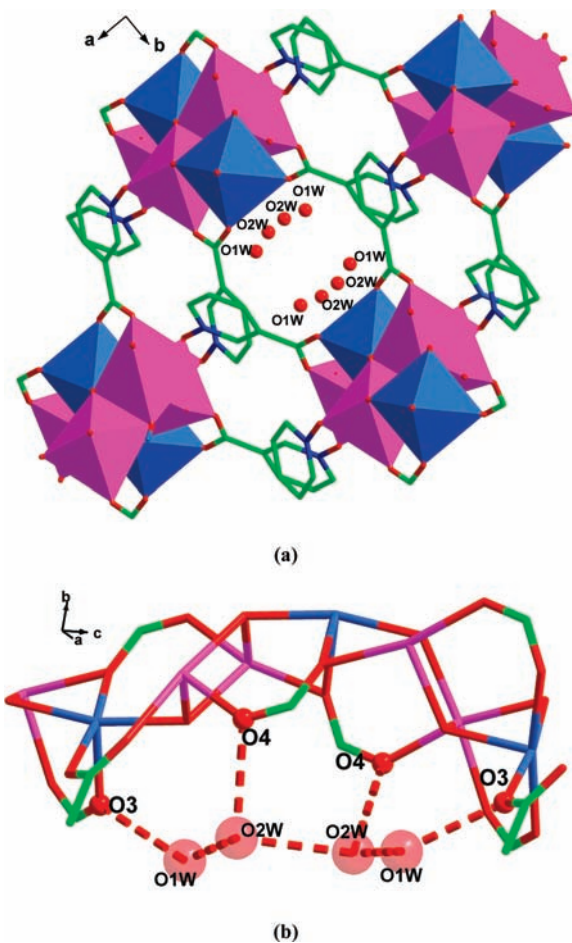


Figure 4. (a) 1D channels of **2** along c filled by water. (b) Hydrogen bonds formed by the included $(\text{H}_2\text{O})_4$ and oxygen atoms of the ligand.

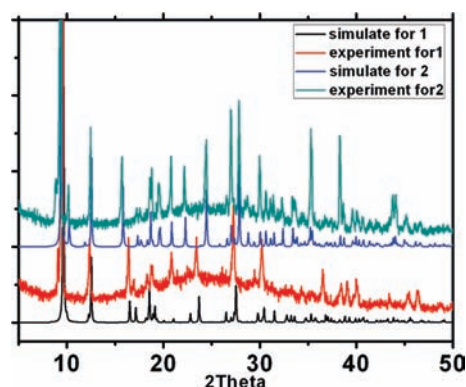


Figure 5. Simulated and experimental XRPD patterns for complexes **1** and **2**.

Magnetic Studies. Magnetic measurements have been carried out on crystalline samples of complexes **1** and **2**. The obtained data indicate dominant antiferromagnetic coupling between the Mn^{II} ions in **1** and **2**. However, in the low-temperature region they show different magnetic behaviors, as discussed below. The magnetic susceptibilities of **1** and **2** were measured in the 2–300 K temperature range under 1 kOe and were shown as $\chi_m T$ versus T plots in Figure 6a. Fitting the data at 50–300 K with the Curie–Weiss law gives $C = 14.1 \text{ cm}^3 \text{ K mol}^{-1}$, $\theta =$

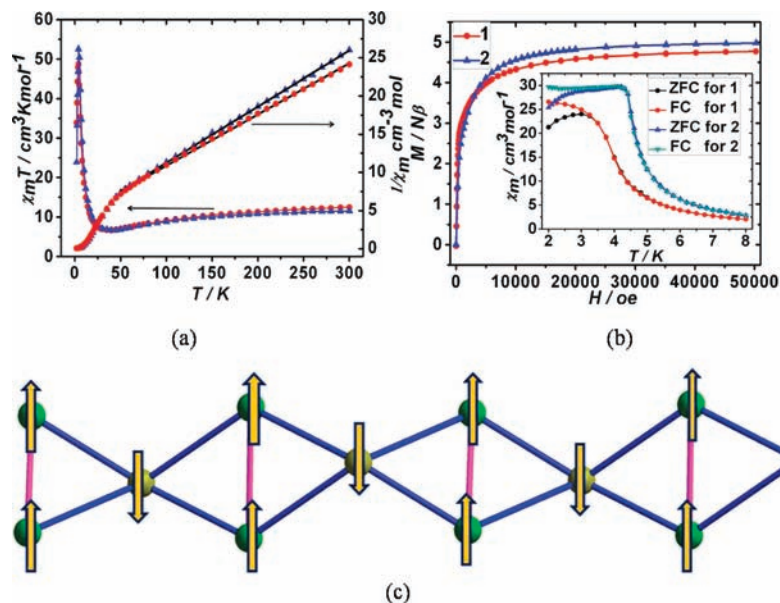


Figure 6. (a) Thermal variation of $\chi_m T$ of **1** (—●—) and **2** (—▲—) at 1 kOe and Curie plot of **1** (●) and **2** (▲). The solid line (—) is the best fit to the Curie–Weiss law. (b) Magnetization vs field plot at 2.0 K of **1** and **2**. Inset: ZFC and FC curves of **1** and **2**. (c) Proposed schematic representation of the spin alignment in the chain of **1** and **2**. The pink lines indicate the ferromagnetic coupling and the light blue antiferromagnetic coupling.

–62.21 K for **1** and $C = 13.59 \text{ cm}^3 \text{ K mol}^{-1}$, $\theta = -52.93 \text{ K}$ for **2** (Figure 6a). The C values are consistent with the value $13.1 \text{ cm}^3 \text{ K mol}^{-1}$ of three noninteracting Mn^{II} ions with $g = 2.0$. The negative value of θ and the initial decrease of $\chi_m T$ should be due to the overall antiferromagnetic coupling between the Mn^{II} ions. Upon further decrease of temperature, however, at 4 K the $\chi_m T$ rises rapidly to maximum values of $48.68 \text{ cm}^3 \text{ K mol}^{-1}$ for **1** and $52.51 \text{ cm}^3 \text{ K mol}^{-1}$ for **2** and finally drops rapidly due to saturation effect. The step rises in $\chi_m T$ at low temperature indicate long-range order in the two complexes. The shape of the $\chi_m T$ versus T plot, with its minimum, is typical of ferrimagnetic behavior or spin canting.¹⁸

The isothermal field-dependent magnetizations $M(H)$ at 2 K at fields up to 50 kOe (Figure 6b) were measured for both **1** and **2**. The field dependence of the magnetization does not follow a Brillouin curve. As shown in Figure 6b, the curves rise sharply to saturation values of $4.8 \text{ N}\beta$ for **1** and $5.0 \text{ N}\beta$ for **2**, in agreement with an uncompensated $S = 5/2$ per one unit. It is consistent with a less common form of ferrimagnetism, namely, homometallic ferrimagnetism, where equal spins are antiparallel but do not cancel overall. The possibility of magnetic transitions suggested by the sharp peaks in the $\chi_m T$ curves was further investigated by measuring the zero-field-cooled (ZFC) and field-cooled (FC) magnetizations in the 1.8–8 K temperature range (Figure 6b, inset). The ZFC/FC measurements were carried out at a very low field of 10 Oe for **1** and **2**. The two curves are superposed at higher temperatures for both compounds (Figure 6b, inset). They increase abruptly below 5 K and then diverge at around 3.2 and 4.0 K for **1** and **2**, respectively. To further probe the long-range ordering in **1** and **2**, the ac magnetic susceptibility measurements were performed with different ac frequencies (Figure 7). The ac susceptibility measurements of **1** in an oscillating field 3 Oe at 10, 100, and

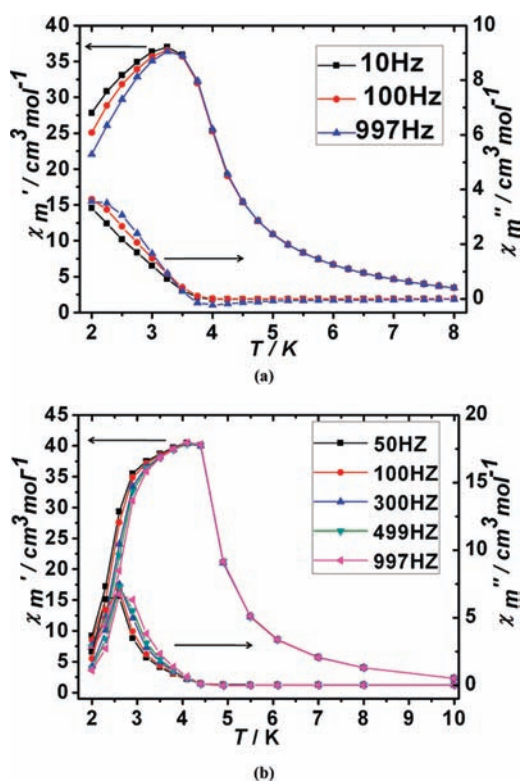


Figure 7. The ac magnetic susceptibility plot at different frequencies: (a) for **1** and (b) for **2**.

997 Hz also indicate a magnetic phase transition occurred below 3 K because both in-phase χ_m' and out-of-phase χ_m'' were observed around this temperature. A peak at 3.3 K of the in-phase χ_m' was observed, but no peak of the χ_m'' curve was present, indicating the phase transition temperature is lower than 2 K (Figure 7a). Different from **1**, the ac magnetic susceptibility measurements of **2** were performed with ac frequencies between 50 and 1000 Hz in

(18) Kahn, O. *Molecular Magnetism*; VCH: New York, 1993.

an oscillating field 2.5 Oe (Figure 7b). The in-phase χ_m' and out-of-phase χ_m'' curves all show peaks that indicate a magnetic phase transition occurred below this temperature. The peaks in ac susceptibilities are sharper for **2** than for **1**, which might be due to a disorder effect. Both the in-phase χ_m' and out-of-phase χ_m'' have a small frequency dependence, but the positions of the peaks χ_m' corresponding to the temperature are constant in the ac measurements, indicating that the single-chain magnetic behavior is not significant in **1** and **2**.¹⁹ Similar examples have also been found in recently reported heterometallic ferrimagnetic systems.²⁰ No significant hysteresis was found in **2** at 2 K (Figure S3). It is like that in the complex the moments within the chain order first and then the 3D ordering take place. However the 3D ordering take place below 2 K, beyond the capability of the squid machine to see any hysteresis.

Complexes **1** and **2** are unusual examples of homospin ferrimagnets. The main superexchange pathway present in **1** (or **2**) is the formate/carboxylate/methoxy (or hydroxyl for **2**) bridges in the chains, and the interchain coupling conducted by the **L** ligands are weak. The coupling that is mediated by double bridges in the *syn*, *syn* formate, and the oxygen of the methoxy (or hydroxyl for **2**) between the Mn1 and Mn2 ions is expected to be antiferromagnetic, as that provides a small metal–metal distance and results in a good overlap of the magnetic orbitals.²¹ The other superexchange pathway between the Mn1 and Mn2 are tripartite bridges, which is the *syn*, *syn* carboxylate and the double oxygen atoms of the formate and methoxy (or hydroxyl for **2**) groups. The cooperative effect of the ternary bridges results in antiferromagnetic coupling. The coupling between two neighboring Mn2 ions bridged by the double oxygen atoms of two methoxy (or hydroxyl for **2**) groups is ferromagnetic. The ferromagnetic coupled Mn2 dimer is antiferromagnetic coupled with neighboring Mn1 ions, leading to the non-compensation in spin moments of Mn^{II} ions (Figure 2a and Figure 6c). However, that is only a proposed model in Figure 6c, and the real magnetic structure needs further confirmation by neutron diffraction. This corresponds

with the ferrimagnetic character of **1** and **2**; otherwise frustration or ferromagnetism would be expected. The magnitude of the coupling constants in the 3D networks of **1** and **2** cannot be calculated by conventional methods.²² Even if only the 1D formate/carboxylate/methoxy (or hydroxyl) Mn^{II} chain was taken into account, there is no appropriate mode for such an arrangement of the spins (Figure 6c).^{5d} The magnetic exchange situations between Mn^{II} ions in **1** and **2** are similar; only one oxygen atom is the methoxy anion in **1** and hydroxyl anion in **2**, which results in the small difference of the magnetic phase transition temperature.

Conclusion

A 3D complex **1** with 3,6-connected 5-nodal net topology was obtained through solvothermal reaction of the manganese formate with nicotinate *N*-oxide in methanol solvent. Complex **1** is formed by formate/carboxylate/methoxy mixed coordinated Mn^{II} chains linked by the **L** ligands. By placing **1** in air for ca. one month, a single-crystal-to-single-crystal structural transition occurred, and the methoxy anions in **1** were replaced by hydroxyl anions and the channels were filled with water molecules, forming another complex, **2**, with similar structure. Magnetic studies reveal that **1** and **2** are both unusual examples of homospin ferrimagnets. The structural differences between complexes **1** and **2** result in the difference of the magnetic phase transition temperature.

Acknowledgment. This work was supported by the 973 Program of China (2007CB815305), the NNSF of China (50673043 and 20773068), and NSF of Tianjin, China (07JCZDJC00500). We thank Prof. You Song and Prof. Ming-Hua Zeng for the measurement and discussion on the magnetic properties.

Note Added after ASAP Publication. This paper was published ASAP on June 22, 2009, with an incorrect version of refs 1b and 11d. The references were corrected, and the paper was reposted on June 25, 2009.

Supporting Information Available: X-ray crystallographic data for complexes **1** and **2** in CIF format and Figures S1–S3. These materials are available free of charge via the Internet at <http://pubs.acs.org>.

(19) Wen, H.-R.; Wang, C.-F.; Li, Y.-Z.; Zuo, J.-L.; Song, Y.; You, X.-Z. *Inorg. Chem.* **2006**, *45*, 7032.

(20) (a) Li, J.-R.; Yu, Q.; Sañudo, E. C.; Tao, Y.; Song, W.-C.; Bu, X.-H. *Chem. Mater.* **2008**, *20*, 1218. (b) Li, D.; Zheng, L.; Zhang, Y.; Huang, J.; Gao, S.; Tang, W. *Inorg. Chem.* **2003**, *42*, 6123. (c) Withers, J. R.; Li, D.; Triplet, J.; Ruschman, C.; Parkin, S.; Wang, G.; Yee, G. T.; Holmes, S. M. *Inorg. Chem.* **2006**, *45*, 4307.

(21) (a) Rodriguez-Forteza, A.; Alemany, P.; Alvarez, S.; Ruiz, E. *Chem.—Eur. J.* **2001**, *7*, 627. (b) Maji, T. K.; Sain, S.; Mostafa, G.; Lu, T.-H.; Ribas, J.; Monfort, M.; Chaudhuri, N. R. *Inorg. Chem.* **2003**, *42*, 709.

(22) (a) Hatfield, W. E. In *Magneto-Structural Correlations in Exchange Coupled Systems*; Willet, R. D., Gatteschi, D., Kahn, O., Eds.; Reidel: Dordrecht, The Netherlands, 1984; p 555. (b) Zeng, M.-H.; Wu, M.-C.; Liang, H.; Zhou, Y.-L.; Chen, X.-M.; Ng, S.-W. *Inorg. Chem.* **2007**, *46*, 7241.